Phase-transition kinetics of magnetic skyrmions investigated by stroboscopic small-angle neutron scattering

Taro Nakajima,[1,*] Yasuhiro Inamura,[2] Takayoshi Ito,[3] Kazuki Ohishi,[3] Hiroshi Oike,[1,4] Fumitaka Kagawa,[1,4] Akiko Kikkawa,[1] Yasujiro Taguchi,[1] Kazuhisa Kakurai,[1,3] Yoshinori Tokura,[1,4] and Taka-hisa Arima[1,5]

[1]*RIKEN Center for Emergent Matter Science (CEMS), Saitama 351-0198, Japan*

[2]*J-PARC Center, Japan Atomic Energy Agency, Tokai, Ibaraki 319-1195, Japan*

[3]*Neutron Science and Technology Center, Comprehensive Research Organization for Science and Society (CROSS), Tokai, Ibaraki 319-1106, Japan*

[4]*Department of Applied Physics and Quantum Phase Electronics Center (QPEC), University of Tokyo, Tokyo 113-8656, Japan*

[5]*Department of Advanced Materials Science, University of Tokyo, Kashiwa 277-8561, Japan*

(Received 4 April 2018; revised manuscript received 1 June 2018; published 23 July 2018)

We investigated the phase-transition kinetics of magnetic skyrmion lattice (SkL) in MnSi by means of stroboscopic small-angle neutron scattering (SANS). Temporal evolutions of SANS patterns were measured with time resolution of 13 ms while sweeping temperature as fast as 50 Ks^{-1}. It turned out that the paramagnetic-to-SkL transition immediately occurs upon traversing the equilibrium phase boundary on the rapid cooling, whereas the SkL-to-conical transition can be kinetically avoided to realize the low-temperature metastable SkL with a long-range magnetic order. The formation of the metastable SkL was found to be strongly dependent not only on cooling rate, but also on magnetic field and trajectory in the H-T phase diagram.

DOI: 10.1103/PhysRevB.98.014424

I. INTRODUCTION

Topologically stable particle-like field configurations have attracted considerable attention in the research fields of nuclear physics [1], quantum Hall systems [2], liquid crystals [3], etc. Among them, magnetic skyrmions, which are nanometric vortex-like magnetic objects in long-wavelength helimagnets, have been intensively investigated for recent years [4–11]. This is partly because they are countable magnetic particles which can be driven by an electric current of low density [12,13]. These characteristics are potentially applicable for new magnetic memory devices [14,15]. Their topological properties are guaranteed as long as the arrangement of magnetic moments in the system is treated as a continuous vector field. In this limit, the magnetic skyrmions are regarded as topological defects, which cannot be removed by adiabatic deformations, and endowed with topological stability. However, real skyrmion-host materials exhibit paramagnetic phases at high temperatures, where a time-averaged amplitude of the local magnetization is zero due to thermal agitation and the skyrmionic order can hardly exist. In bulk samples, most of the skyrmion phases have two kinds of phase boundaries: one is facing another magnetically ordered (mostly conical magnetic) phase, and the other is facing a paramagnetic (or fluctuation-disordered [16]) phase. On these boundaries, the validities of the topological stability should be different from each other.

This difference may be manifested in the kinetics of phase transitions with varying temperature. An example is the thermal quenching process of the skyrmion lattice state in MnSi [17,18]. A metallic helimagnet, MnSi exhibits a skyrmion lattice (SkL) phase only in a very narrow temperature and magnetic field window just below the transition temperature of $T_C = 29$ K [5]. However, a recent Hall resistivity measurement demonstrated that the thermoequilibrium SkL state can be quenched to low temperatures, so it can persist as a metastable state in a wider temperature and magnetic field range [17]. In the previous study, an electric current pulse was applied to a MnSi single crystal at a low temperature in a magnetic field. The sample was heated above T_C due to the Joule heating, and then it was rapidly cooled to the base temperature passing through the equilibrium SkL state. Although the system originally exhibits a conical magnetic order at low temperatures, the SkL-to-conical phase transition can be kinetically avoided upon the rapid cooling. A recent small-angle neutron scattering (SANS) study also confirmed that the quenched skyrmions still maintain the triangular lattice form [19]. In both the experiments, however, the metastable SkL was evidenced by comparing the Hall resistivity or SANS patterns measured in the respective steady states before and after a current pulse application. It is not yet clear how dynamically the phase transitions proceed during the current pulse application.

To investigate the phase-transition kinetics in MnSi upon rapid cooling, a real-time observation of the magnetic order is necessary. One of the possible approaches is a "pump-and-probe" or "stroboscopic" time-resolved measurement [20–25]. In the present study, we performed a stroboscopic SANS experiment on a single crystal of MnSi at a time-of-flight (TOF) neutron scattering instrument TAIKAN (BL15) in the pulsed neutron source of materials and life science facility (MLF) in J-PARC [26]. By synchronizing electric current and neutron pulses, we implemented the stroboscopic approach in the TOF neutron scattering instrument, which enables us to observe temporal evolutions in neutron scattering patterns with a time

*taro.nakajima@riken.jp

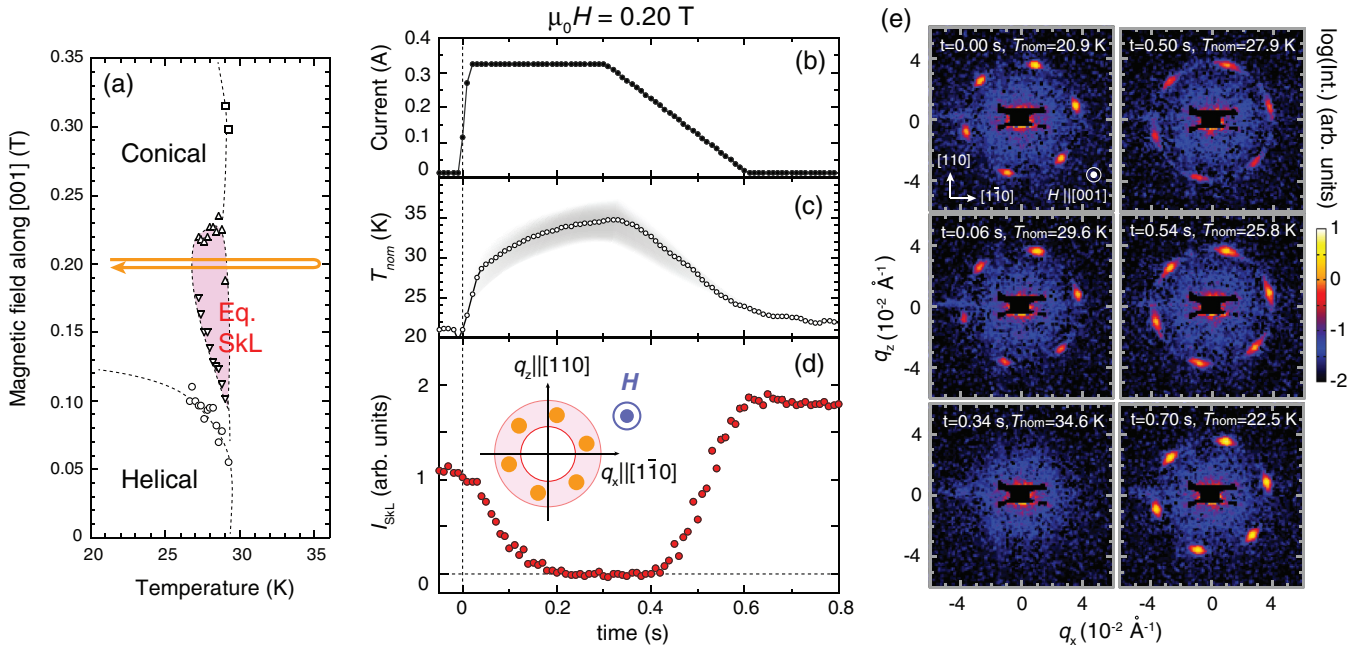

FIG. 1. (a) H-T magnetic phase diagram of MnSi for magnetic fields along the [001] axis (redrawn from the data presented in Ref. [19]). Time profiles of the (b) electric current pulse, (c) nominal temperature $T_{\rm nom}$, and (d) integrated intensity of the magnetic Bragg reflections from the SkL order, $I_{\rm SkL}$. Inset schematically shows the integrated area. (e) Typical SANS patterns at selected time frames during the current pulse applications.

resolution of 13 ms (see the Supplemental Material for details of the experimental setup and the time resolution [27]).

II. RESULTS AND DISCUSSIONS

First, we investigated the kinetics of magnetic phase transitions in a magnetic field of 0.2 T along the [001] axis. We applied electric current pulses at 21.5 K, which is far below the equilibrium SkL phase, as shown in Fig. 1(a). Figure 1(b) shows a time profile of the electric current pulse with a height of 323 mA. The current density in the sample is calculated to be 2.2×10^5 A m^{-2}, which does not cause irreversible unwinding of metastable skyrmions [28]. The sample temperature was deduced from the resistivity measured during the current pulse application, in the same manner as in the previous studies [17–19]. As shown in Fig. 1(c), the sample was heated up to approximately 35 K, and then rapidly cooled down to the base temperature at a rate of 50 K s^{-1}. We repeated the current pulse application approximately 1000 times, and accumulated the SANS signals for each time frame. Figure 1(e) shows the temporal evolution of the SANS pattern during the rapid temperature sweeping. At $t = 0$, a hexagonal diffraction pattern is observed on a plane perpendicular to the magnetic field. This corresponds to the triangular lattice of metastable skyrmions, which was already created by repeating current pulses. The magnetic Bragg reflections disappeared once at high temperatures [e.g., $t = 0.34$ s in Fig. 1(e)], and then reappeared on the subsequent cooling (e.g., $t \geqslant 0.5$ s), as also evidenced by temporal evolution of integrated intensity of the magnetic reflections shown in Fig. 1(d).

We noticed that a nonzero intensity remains in the time ranges of $t = 0.07$–0.20 s and $t = 0.40$–0.47 s, where the system is supposed to be in the paramagnetic phase at thermal equilibrium. A finite-element calculation of the thermal distribution suggests that the actual temperature of the sample was not uniform but had some distribution, as schematically illustrated by a gray shaded area in Fig. 1(c) (see Supplementary Fig. S3 for details), which blurred the time profile of the integrated intensity. In this paper, we thus refer to the temperature deduced from the transient resistivity value as the nominal temperature, $T_{\rm nom}$.

Here, we focus on the rapid cooling process, which corresponds to the time range of $t = 0.3$–0.7 s, to investigate how the skyrmions are formed from the paramagnetic phase and finally quenched to low temperatures. We extracted the integrated intensity ($I_{\rm SkL}$), length of the Q vector ($|Q|$), and half widths at the half maximum of the magnetic Bragg reflections along the radial and azimuthal directions ($w_\parallel$, $w_\perp$), from the SANS patterns at each elapsed time t. Figures 2(a)–2(d) show these parameters as functions of $T_{\rm nom}$. We also measured the SANS patterns on slow cooling without applying electric current pulses, and plotted the parameters in these figures as functions of T. We found that $I_{\rm SkL}$ started to grow at $T_{\rm nom} = 31$ K upon rapid cooling. Taking into account the difference between the nominal and actual temperatures, we concluded that the paramagnetic-to-SkL phase transition takes place at around T_C even upon rapid cooling, revealing that the formation of skyrmions is fast enough to follow the rapid change in temperature due to the infinitesimal ordered moment at the T_C. Upon further cooling, $I_{\rm SkL}$ monotonically increases even in the metastable regime, indicating that the magnitude of the ordered magnetic moments is still developing from the value of the equilibrium state.

Another parameter to describe the magnetic order is $|Q|$, which represents, in a helimagnet, a turning angle between neighboring magnetic moments. A previous SANS study on

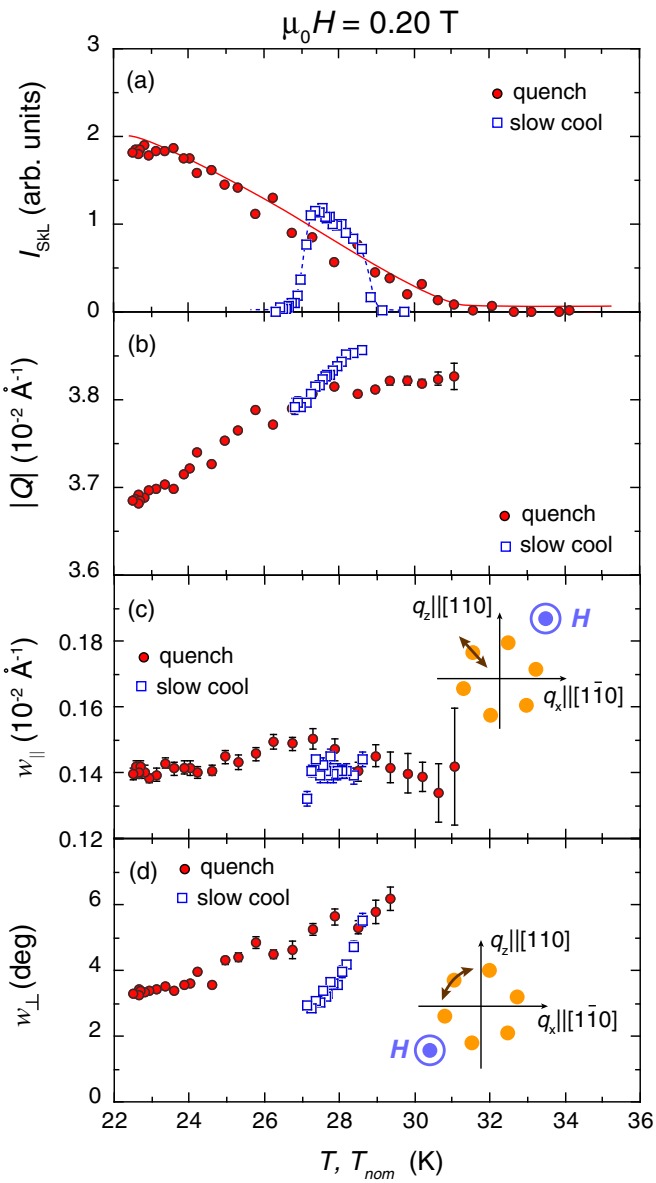

FIG. 2. $T_{\rm nom}$ and T variations of (a) $I_{\rm SkL}$, (b) length of the magnetic modulation wave vector $|Q|$, and half-widths of the half maximum of the Bragg reflections along the (c) radial and (d) azimuthal directions. Solid and dashed lines in (a) are guides to the eyes. Insets in (c) and (d) schematically show the relationships between the crystallographic and magnetic field directions and the radial and azimuthal directions in the reciprocal lattice space, respectively.

MnSi reported that $|Q|$ decreased with decreasing temperature in the helical phase [29]. In the present experiment, $|Q|$ of the SkL state also decreases on rapid cooling, and coincides with the value measured on slow cooling at around 27 K, as shown in Fig. 2(b). Interestingly, $|Q|$ keeps decreasing from the value of the equilibrium SkL phase with decreasing temperature. This is in sharp contrast to a previous SANS study on SkL in (Fe,Co)Si [30], which is also known to exhibit a metastable SkL state on cooling in a magnetic field. In (Fe,Co)Si, the temperature evolution of $|Q|$ was stopped when the system entered the metastable regime. It was concluded that the metastability of the SkL state in (Fe,Co)Si is mainly attributed to a pinning effect due to the chemical disorder, namely, random distribution of Fe and Co. By contrast, the present results show that magnetic moments gradually change their turning angle even in the metastable SkL state. We thus conclude that the pinning effect due to chemical disorder is less effective in MnSi, suggesting that the metastabilization of the SkL state in MnSi is governed mainly by a competition between the cooling speed and the time scale of the topological unwinding of the skyrmions.

We also found that the metastable SkL appeared as a long-range magnetic order at the lowest temperature. As shown in Figs. 2(c) and 2(d), $w_{\parallel}$ and $w_{\perp}$ decrease on rapid cooling, respectively, and finally become comparable with the minimum widths obtained in slow cooling, indicating that the metastable skyrmions are arranged in a regular triangular lattice on the plane perpendicular to the field [see Supplemental Material and Supplementary Fig. S4 for more details on the formation of the long-range order (LRO)]. One should note here that information about the out-of-plane magnetic correlation is still lacking in the present study. To investigate this point, it will be necessary to combine the stroboscopic SANS measurements and rocking scans.

Another point to be noted here is that in the temperature range of $27 < T_{\rm nom} < 28$ K, where the $|Q|$ rapidly changes on quenching, $w_{\parallel}$ and $w_{\perp}$ were larger than those on the slow cooling, as seen in Figs. 2(c) and 2(d). We infer that the T variation of $|Q|$ introduces some imperfections in the SkL order; because the number of topological particles tends to be conserved in the limited volume of the sample, the rapid reduction in $|Q|$, which means rapid increase of the core-to-core distance between neighboring skyrmions, may result in temporal disorder or dislocation in the arrangement of the skyrmion particles, though they are finally rearranged to achieve the LRO at the lowest temperature.

Having established the kinetics of phase transitions at 0.2 T, we investigated how they depend on the magnetic field. Figures 3(a) and 3(b) show time profiles of $I_{\rm SkL}$ and their variations as a function of $T_{\rm nom}$ with varying magnetic field, respectively. Here, we also show integrated intensities of the conical phase, I_C, which were measured by rotating the sample and direction of the magnetic field by 90° about the vertical axis. At each magnetic field, the current pulse application was repeated for 300–1000 times. The integrated area for I_C is schematically shown in Fig. 3(c). Importantly, the paramagnetic-to-SkL phase transition was detected at all the magnetic fields, supporting our conclusion that the formation of the SkL is quite fast and immediately occurs at the critical temperature. On the other hand, the SkL-to-conical phase transition strongly depends not only on cooling rate, but also on magnetic field. In particular, at 0.15 and 0.22 T, the metastable SkL state was not observed at the lowest temperature. The SkL state turns into the equilibrium conical phase even upon the rapid cooling at a cooling rate of 50 K s^{-1}. Note that even at 0.2 T, there is a temporal decay of the metastable SkL state in the time range from 1 to 10 s, as shown in Fig. 3(a), showing that the metastable SkL has a finite lifetime at this temperature (22 K).

One may consider that the metastable SkL would no longer be stable at 0.15 and 0.22 T, which is, however, not the case. In Fig. 3(d), we show field dependence of $I_{\rm SkL}$ measured after

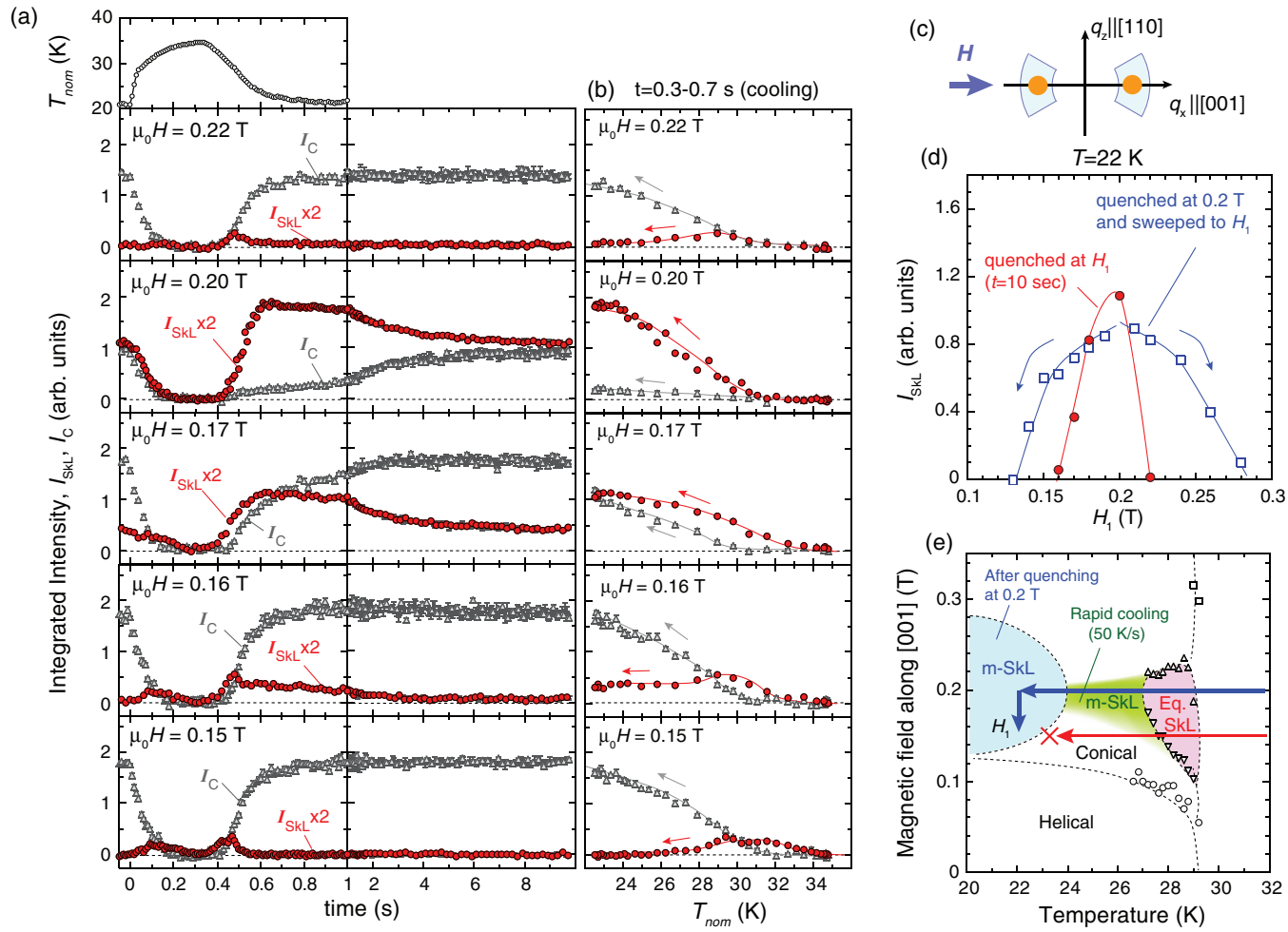

FIG. 3. (a) Temporal profiles of $T_{\rm nom}$, $I_{\rm SkL}$, and I_C measured at a number of magnetic fields. (b) $I_{\rm SkL}$ and I_C replotted as functions of $T_{\rm nom}$. Solid lines are guides to the eyes. (c) Integrated area for magnetic reflections of the conical phase. (d) Magnetic field dependence of $I_{\rm SkL}$ measured in two different paths shown in (b). The lines are guides to the eyes. (e) Metastable state and equilibrium phase diagram of MnSi. The phase boundaries are redrawn from the data presented in Ref. [19]. The light-blue area shows where the metastable SkL state (labeled "m-SkL") has a life time longer than about 10^2 s, once it is created. The green area qualitatively shows the H and T range where the metastable SkL state can temporarily exist upon quenching with the cooling rate of 50 K s^{-1}.

quenching at 0.2 T; we created the metastable SkL at 0.2 T and 22 K, swept the magnetic field to H_1, as illustrated by blue arrows in Fig. 3(e), and then measured SANS patterns. The typical data acquisition time was about 5 min. We detected sizable intensities at 0.15 and 0.22 T, revealing that once the metastable SkL is created, it persists (at least for more than 10 s) in a wide magnetic field range from 0.13 to 0.28 T, at 22 K. Nonetheless, it cannot be reached from the quenching process at a fixed magnetic field, e.g., 0.13 and 0.28 T, other than the optimum one (0.2 T).

These observations provide insights into how the equilibrium SkL phase is connected to the metastable SkL state. The present cooling rate of 50 K s^{-1} can quench the equilibrium SkL state to low temperatures only in a narrow window of magnetic field near 0.2 T, as indicated a green area in Fig. 3(e). This is quite reasonable because the transition temperature from the equilibrium SkL phase to the conical phase is minimized at around 0.2 T (see Fig. 1(a)). By minimizing the thermal fluctuation, the system can pass through the equilibrium phase boundary while keeping the topology of spin texture. As increasing or decreasing magnetic field from 0.2 T, the SkL-to-conical phase boundary is shifted toward higher temperatures, where the thermal fluctuations become stronger. As a result, the cooling rate of 50 K s^{-1} is still not fast enough to kinetically avoid the transformation of the magnetic order from the SkL to conical states. Accordingly, it can be expected that the window of magnetic field needed to realize the metastable SkL states is expanding with increasing cooling rate. In fact, in the previous Hall resistivity measurements on MnSi upon a more rapid quenching at a cooling rate of approximately 700 K s^{-1} [17], the thermal quenching of the SkL state was possible in a wider range of magnetic field, which covers the whole area of equilibrium SkL phase.

III. SUMMARY

In summary, we have investigated the phase-transition kinetics of the SkL in MnSi upon a rapid cooling by means of stroboscopic SANS measurements. We found that the paramagnetic-to-SkL transition occurs when traversing the

equilibrium phase boundary, indicating that the creation of the skyrmions is fast enough to follow the temperature change of 50 K s^{-1}. By contrast, the SkL-to-conical transition was found to be strongly dependent not only on the cooling rate, but also on the magnetic field and trajectory in the phase diagram. At 0.2 T, where the equilibrium SkL-to-conical transition temperature is minimized, the transition is completely avoided by the rapid cooling of 50 K s^{-1}, and finally the metastable SkL state exhibits a magnetic LRO at low temperatures. The length of the Q vector keeps on changing with decreasing temperature in the metastable SkL state, suggesting that the metastabilization of the SkL state in MnSi is governed not by a pinning effect due to chemical disorder, but by a competition between the cooling speed and the time scale of the topological unwinding of the skyrmions. We also emphasize that the stroboscopic SANS technique will be a powerful tool to explore the ordering kinetics and transient phenomena of magnetic skyrmions and other topological spin textures.

ACKNOWLEDGMENTS

The SANS experiment at the Materials and Life Science Experimental Facility of the J-PARC was performed under a user program (Proposals No. 2017A0155 and No. 2016C0002). This work was partially supported by JSPS KAKENHI (Grant No. 25220709).

[1] T. H. Skyrme, Nucl. Phys. **31**, 556 (1962).
[2] S. L. Sondhi, A. Karlhede, S. A. Kivelson, and E. H. Rezayi, Phys. Rev. B **47**, 16419 (1993).
[3] J.-i. Fukuda and S. Žumber, Nat. Commun. **2**, 246 (2011).
[4] U. K. Rößler, A. N. Bogdanov, and C. Pfleiderer, Nature **442**, 797 (2006).
[5] S. Mühlbauer, B. Binz, F. Jonietz, C. Pfleiderer, A. Rosch, A. Neubauer, R. Georgii, and P. Böni, Science **323**, 915 (2009).
[6] W. Münzer, A. Neubauer, T. Adams, S. Mühlbauer, C. Franz, F. Jonietz, R. Georgii, P. Böni, B. Pedersen, M. Schmidt *et al.*, Phys. Rev. B **81**, 041203 (2010).
[7] X. Z. Yu, Y. Onose, N. Kanazawa, J. H. Park, J. H. Han, Y. Matsui, N. Nagaosa, and Y. Tokura, Nature **465**, 901 (2010).
[8] S. Seki, X. Z. Yu, S. Ishiwata, and Y. Tokura, Science **336**, 198 (2012).
[9] N. Nagaosa and Y. Tokura, Nat. Nanotech. **8**, 899 (2013).
[10] I. Kézsmárki, S. Bordacs, P. Milde, E. Neuber, L. M. Eng, J. S. White, H. M. Ronnow, C. D. Dewhurst, M. Mochizuki, K. Yanai *et al.*, Nat. Mater. **14**, 1116 (2015).
[11] Y. Tokunaga, X. Z. Yu, J. S. White, H. M. Ronnow, D. Morikawa, Y. Taguchi, and Y. Tokura, Nat. Commun. **6**, 8638 (2015).
[12] F. Jonietz, S. Mühlbauer, C. Pfleiderer, A. Neubauer, W. Münzer, A. Bauer, T. Adams, R. Georgii, P. Böni, R. A. Duine *et al.*, Science **330**, 1648 (2010).
[13] X. Yu, N. Kanazawa, W. Zhang, T. Nagai, T. Hara, K. Kimoto, Y. Matsui, Y. Onose, and Y. Tokura, Nat. Commun. **3**, 988 (2012).
[14] W. Koshibae, Y. Kaneko, J. Iwasaki, M. Kawasaki, Y. Tokura, and N. Nagaosa, Jpn. J. Appl. Phys. **54**, 053001 (2015).
[15] A. Fert, V. Cros, and J. Sampaio, Nat. Nanotech. **8**, 152 (2013).
[16] M. Janoschek, M. Garst, A. Bauer, P. Krautscheid, R. Georgii, P. Böni, and C. Pfleiderer, Phys. Rev. B **87**, 134407 (2013).
[17] H. Oike, A. Kikkawa, N. Kanazawa, Y. Taguchi, M. Kawasaki, Y. Tokura, and F. Kagawa, Nat. Phys. **12**, 62 (2016).
[18] F. Kagawa and H. Oike, Adv. Mater. **29**, 1601979 (2017).
[19] T. Nakajima, H. Oike, A. Kikkawa, E. P. Gilbert, N. Booth, K. Kakurai, Y. Taguchi, Y. Tokura, F. Kagawa, and T.-h. Arima, Sci. Adv. **3**, e1602562 (2017).
[20] N. Niimura and M. Muto, Nucl. Instrum. Methods **126**, 87 (1975).
[21] H. Nojiri, M. Motokawa, N. Nishida, and Y. Endoh, Physica B **180-181**, 31 (1992).
[22] A. Wiedenmann, U. Keiderling, K. Habicht, M. Russina, and R. Gähler, Phys. Rev. Lett. **97**, 057202 (2006).
[23] S. Mühlbauer, J. Kindervater, T. Adams, A. Bauer, U. Keiderling, and C. Pfleiderer, New J. Phys. **18**, 075017 (2016).
[24] K. Litzius, I. Lemesh, B. Krüger, P. Bassirian, L. Caretta, K. Richter, F. Büttner, K. Sato, O. A. Tretiakov, J. Förster *et al.*, Nat. Phys. **13**, 170 (2016).
[25] G. Berruto, I. Madan, Y. Murooka, G. M. Vanacore, E. Pomarico, J. Rajeswari, R. Lamb, P. Huang, A. J. Kruchkov, Y. Togawa *et al.*, Phys. Rev. Lett. **120**, 117201 (2018).
[26] S. Takata, J. Suzuki, T. Shinohara, T. Oku, T. Tominaga, K. Ohishi, H. Iwase, T. Nakatani, Y. Inamura, T. Ito *et al.*, JPS Conf. Proc. **8**, 036020 (2015).
[27] See Supplemental Material at http://link.aps.org/supplemental/10.1103/PhysRevB.98.014424 for details of the experiments and the time resolution of the stroboscopic SANS measurements.
[28] F. Kagawa, H. Oike, W. Koshibae, A. Kikkawa, Y. Okamura, Y. Taguchi, N. Nagaosa, and Y. Tokura, Nat. Commun. **8**, 1332 (2017).
[29] S. V. Grigoriev, S. V. Maleyev, A. I. Okorokov, Y. O. Chetverikov, P. Böni, R. Georgii, D. Lamago, H. Eckerlebe, and K. Pranzas, Phys. Rev. B **74**, 214414 (2006).
[30] L. J. Bannenberg, K. Kakurai, F. Qian, E. Leliévre-Berna, C. D. Dewhurst, Y. Onose, Y. Endoh, Y. Tokura, and C. Pappas, Phys. Rev. B **94**, 104406 (2016).